Analytical Expressions for Spherical Wire Antenna Quality Factor Demonstrating Exact Agreement Between Circuit-Based and Field Integration Techniques

Alexander B. Murray, *Graduate Student Member, IEEE*, and Ashwin K. Iyer, *Senior Member, IEEE*

***Abstract*— Properties of spherical wire antennas are revisited using a circuit analysis approach. This methodology yields the exact quality factor and axial ratio (AR) of coupled-mode spherical radiators as analytical expressions. The new circuit-based equations are compared to field integration predictions for quality factor, and both are found to agree for a general multipole expansion of the electromagnetic fields. These two predictions of stored energy inside a spherical wire antenna are shown to be equivalent via direct analysis, while predictions of stored energy outside the spherical wire antenna are compared by way of mathematical induction. In addition, the circuit analysis reveals general relations between supplied current and radiated power of spherical wire antennas, resonance conditions of coupled-mode systems, and analytical quantification of the trade-off between the quality factor and AR for TM_{1m}–TE_{1m} radiators. New and simple expressions for the minimum quality factor of circular, near-circular, linear, and general elliptical polarizations are provided.**

***Index Terms*— Axial ratio (AR), circular polarization, electrically small antennas (ESAs), quality factor, spherical antennas, spherical wave expansion.**

I. Introduction

THE analysis of spherical waves for determining limitations on electrically small antennas (ESAs) dates back many decades to the work of Chu [1], who constructed equivalent circuits describing the fields of the modes external to what is now known as a Chu sphere. Conventionally, this Chu sphere is taken to have radius a. In practice, these circuits placed limitations on the quality factor (Q), and hence bandwidth, of any passive, linear, and time-invariant antenna circumscribed by this Chu sphere. Collin and Rothschild [2] built on this spherical wave analysis from a field perspective, to obtain the widely used lower bound on radiation Q as follows:

$$Q_{\text{Chu}} = \frac{1}{(ka)^3} + \frac{1}{ka} \tag{1}$$

where k is the wavenumber at resonance, and the radiator is assumed to be perfectly efficient. Equation (1) presumes the presence of only one of the two lowest Q modes (i.e., the TM_{1m} and TE_{1q} modes, which are the lowest Q modes for small ka). In the works that followed, much of the study of ESA performance through the lens of spherical waves has been conducted either by equivalent circuit analysis [3], [4], [5], [6], [7] or through direct field analysis [4], [8], [9], [10]. To date, these two formalisms have only been shown to be in agreement for very low-order spherical waves [2], [4]. While (1) is one of the most commonly cited lower bounds, an antenna radiating both the TM_{1m} and TE_{1q} modes is constrained to the lower bound

$$\hat{Q}_{\text{Chu}} = \frac{1}{2(ka)^3} + \frac{1}{ka} \tag{2}$$

which is derived under the same assumption of only considering the fields outside of the Chu sphere [4]. A lower bound with this same limiting form can be obtained for a single mode if lossy and dispersive tuning is permitted, as shown by Yaghjian [11]. It is worth noting that the limits of ESAs have been estimated outside the context of a spherical wave expansion. To name a few, Gustafsson et al. [12] consider the scattering properties of antennas via their polarizability dyads, a general approach which permits the study of antennas bounded by volumes of arbitrary shape. Yaghjian et al. [13] also deviate from the spherical wave approach to study antennas bounded by volumes of arbitrary shape.

Returning to the circuit perspective of spherical wave theory, Thal [5] extended Chu's circuits to account for the energy in both interior and exterior to the Chu sphere, presuming electric currents flowing only on the surface of the Chu sphere (a description of so-called spherical wire antennas). The modal circuits were extended by first considering the original circuits of Chu generated by the outwardly traveling wave impedances (normalized to the intrinsic impedance of free space) at the

Manuscript received 23 June 2023; revised 16 October 2023; accepted 20 November 2023. Date of publication 6 December 2023; date of current version 15 February 2024. This work was supported in part by the Department of National Defence (DND) through the Innovation for Defence Excellence and Security (IDEaS) Program. *(Corresponding author: Ashwin K. Iyer.)*

The authors are with the Department of Electrical and Computer Engineering, University of Alberta, Edmonton, AB T6G 2R3, Canada (e-mail: abmurray@ualberta.ca; iyer@ece.ualberta.ca).

Color versions of one or more figures in this article are available at https://doi.org/10.1109/TAP.2023.3337946.

Digital Object Identifier 10.1109/TAP.2023.3337946

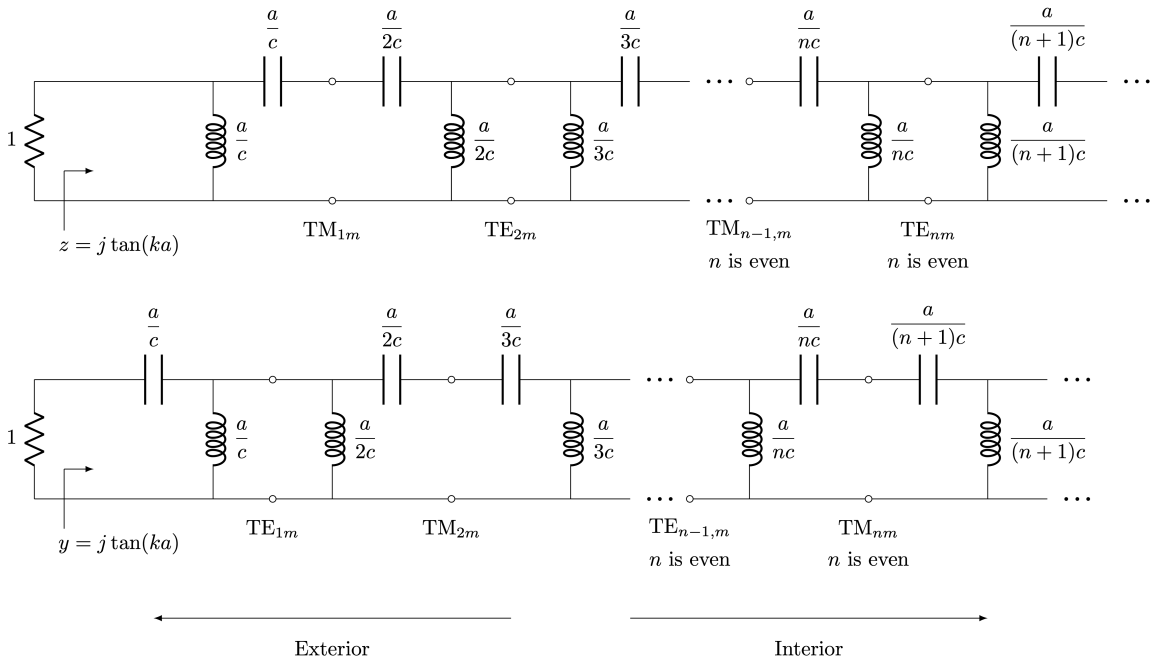

Fig. 1. Exact circuits introduced by Thal [5] for the modes excited by a spherical wire antenna of radius a.

Chu sphere

$$Z_{nm}^{\mathrm{TM}+} = j\frac{\left[ka \cdot h_n^{(2)}(ka)\right]'}{ka \cdot h_n^{(2)}(ka)} \tag{3}$$

for TM waves, and

$$Z_{pq}^{\mathrm{TE}+} = -j\frac{ka \cdot h_p^{(2)}(ka)}{\left[ka \cdot h_p^{(2)}(ka)\right]'} \tag{4}$$

for TE waves, where the primes indicate differentiation with respect to ka. Recurrence relations of the spherical Hankel functions of the second kind $h_n^{(2)}$ were then used to express (3) and (4) as a continued fraction, making the form of the equivalent circuit more obvious. Thal took the same approach that Chu took as outlined above, but performed additional analysis on the inwardly directed wave impedances at the Chu sphere

$$Z_{nm}^{\mathrm{TM}-} = -j\frac{\left[ka \cdot j_n(ka)\right]'}{ka \cdot j_n(ka)} \tag{5}$$

and

$$Z_{pq}^{\mathrm{TE}-} = j\frac{ka \cdot j_p(ka)}{\left[ka \cdot j_p(ka)\right]'} \tag{6}$$

where j_n are the spherical Bessel functions of the first kind, and the impedances are again normalized to the intrinsic impedance of free space. Using the same procedure, networks representing the interior region of a spherical wire antenna were combined with those representing the exterior region as shown in Fig. 1 for each individual spherical mode. Systems supporting multiple modes (hereafter referred to as coupled-mode systems) may be combined with a coupling network, as shown in Fig. 2. The quality factor for any coupled-mode system can then be extracted by computing the stored electric

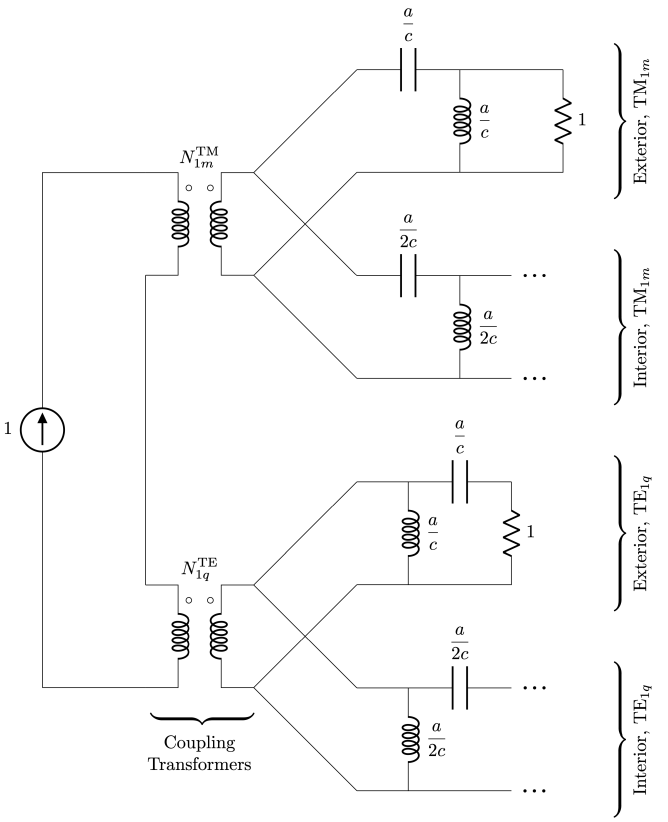

Fig. 2. Circuit for the coupled TM_{1m}–TE_{1q} system introduced by Thal [5].

and magnetic energy in the circuit (W_{e} and W_{m}) and dissipated power P to compute the Q as follows:

$$Q = 2\omega\frac{\max(W_{\mathrm{e}},\ W_{\mathrm{m}})}{P} \tag{7}$$

where ω is the angular frequency. These circuits permit calculation of the radiation Q of material cores by scaling the inductors and capacitors by the relative permeability and permittivity, respectively.

Hansen et al. [9] address the same problem but from the field perspective. By integrating over the fields of the modes, they were able to recover expressions for the interior and exterior stored energies (distinguishing between electric and magnetic energy) as well as the dissipated power, permitting analytical computation of spherical wire antenna Q with material cores. In this article, their air-core results (those results assuming the permittivity and permeability of vacuum inside the Chu sphere) will be shown equivalent to Thal's generalized circuits. In returning to this circuit perspective, these equivalent equations take on different forms. This circuit formalism, validated by the aforementioned field approach, provides analytical tools that easily connect the quality factor and polarization purity of ESAs. This newfound equivalence between circuit and field integration formalisms, as well as new links between quality factor and polarization purity and their associated lower bounds as described by simple expressions, forms the main contributions of this article.

This analysis is primarily focused on coupled-mode antennas, as these are the antennas providing the lowest Q. This motivates a slightly different notation than is typically used; while usual reference to TE modes uses the subscripts n and m, the subscripts p and q will be used to illustrate when the mode indices between coupled TM–TE systems may be different should both appear in the same expression. The use of n and m indices for the TE modes will be reserved for when they must match the TM counterpart. Otherwise, reference to the modes and their definitions are made according to [14], which assumes time-harmonic fields with time dependence $\exp(j\omega t)$. This time dependence is suppressed throughout this article. Furthermore, the analysis focuses on the important special case of air-core antennas carrying electric currents, which do not make use of dispersive tuning; all results and statements herein are made under these simplifications. The arguments for spherical Bessel and Hankel functions are omitted for the remainder of this article, as their argument is always ka.

This article is organized as follows. Section II considers the impedances of the equivalent networks, which yield relations between supplied current and radiated power, as well as resonance conditions for coupled-mode systems. Section III then uses the circuits to analytically compute the axial ratio (AR) and Q of the modes. These results are then used in Section IV to quantify the exact trade-off between Q and polarization purity. The exact circuit results are then shown to be in agreement with the field integration results of [9] in Section V. This article is then concluded in Section VI.

II. Mode Impedances and Resonance Conditions

A. Two-Element Equivalent Circuits

While the physical meaning of mode impedances as used in this section is not shown to be equivalent to usual circuit impedances, they still provide value in the computation of radiated power or resonance conditions of coupled-mode systems. Computing radiated power from the supplied current excitation, and concluding resonance when the reactances are zero, is the extent of the physical meaning verified for the impedances of this section. Whether or not they have any correspondence to the input impedance of an antenna supporting these modes is not proven herein.

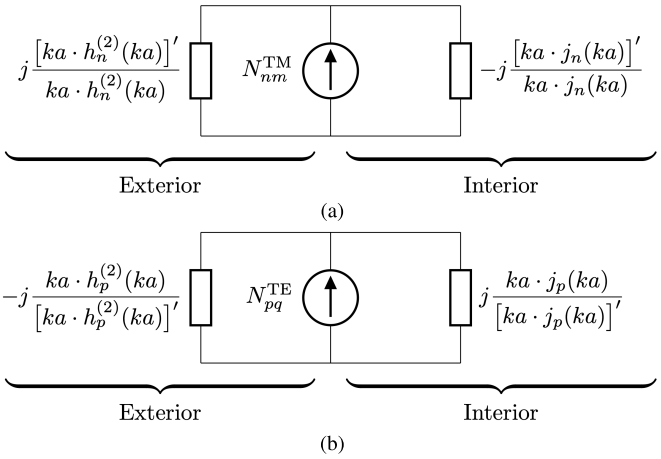

Fig. 3. Equivalent two-element representation of (a) TM_{nm} and (b) TE_{pq} modal circuits.

From the form of the modal circuits accounting for stored energy in the interior and exterior of the Chu sphere shown in Fig. 1, general expressions for the mode impedances are not obvious. However, based on how the circuits were introduced in Section I, an alternative and more compact circuit can be constructed, albeit with elements having impedances of more complicated forms. These circuits are shown in Fig. 3.

Without performing any circuit analysis, sophisticated field integration, or additional normalization of the mode definitions, it is clear from Fig. 3 that no power is delivered to the exterior networks (thus, no power is delivered to the far-field) for TM_{nm} modes at electrical sizes satisfying $(kaj_n)' = 0$, and likewise for the TE_{pq} modes at electrical sizes satisfying $kaj_p = 0$. At these particular electrical sizes, the interior network shorts the current source. Note that in the case of magnetic currents flowing on the surface of the spherical antenna, the shunt current source is replaced with a series voltage source. The nonradiative electrical sizes of magnetic current excitation, thus, occur for the open-circuit conditions of the interior fields, dual to the electric current excitation. Even for the case where no current is delivered to the interior circuit, it can still hold energy, analogous to a parallel LC network at antiresonance, and thus, Q does not reconverge to (1). This conclusion was also reached by [9] after some mathematical manipulation.

B. Mode Impedances

While nulls in the radiated power can easily be found, other quantities of interest, such as the resonant-coupling condition, require a more involved analysis. For these circuits of finitely many elements, closed-form input resistances and reactances can be extracted, which allows for the resonant modal

coupling to be derived for any two sets of modes. For the isolated modes, the input resistances R and reactances X are given by

$$R_{nm}^{\mathrm{TM}} = \left[(kaj_n)'\right]^2 \tag{8}$$

$$R_{pq}^{\mathrm{TE}} = \left(kaj_p\right)^2 \tag{9}$$

$$X_{nm}^{\mathrm{TM}} = -(kaj_n)'(kay_n)' \tag{10}$$

$$X_{pq}^{\mathrm{TE}} = -\left(kaj_p\right)\left(kay_p\right) \tag{11}$$

where y_n is the spherical Bessel function of the second kind. Equation (9) is a generalized and normalized version that was found for a TE_{10} source in [15] via field analysis. These equations for reactance are generalized versions of those in [5]. Equations (8) and (9) permit direct calculation relating far-field power of a mode to its modal coupling, represented by the transformer turn ratios N_{nm}^{TM} and N_{pq}^{TE}. If the far-field power contributions P_{nm}^{TM} and/or P_{pq}^{TE} of particular modes are known, *relative* modal coupling (in the form of transformer turns ratios) can be extracted as follows:

$$N_{nm}^{s} = \sqrt{\frac{P_{nm}^{s}}{R_{nm}^{s}}} \tag{12}$$

where s represents either TM or TE. This relation permits direct calculation of coupled-mode lower bounds on Q in a given simulation or experiment as will be evident in Section III. Equations (10) and (11) can be shown to be in agreement with Thal [5] by considering special cases of their Laurent series expansions about $ka = 0$

$$X_{10}^{\mathrm{TM}} = -\frac{2}{3ka} + \mathcal{O}(ka) \tag{13}$$

$$X_{10}^{\mathrm{TE}} = \frac{ka}{3} + \mathcal{O}\left[(ka)^3\right] \tag{14}$$

$$X_{20}^{\mathrm{TE}} = \frac{ka}{5} + \mathcal{O}\left[(ka)^3\right]. \tag{15}$$

An analytical means of computing these Laurent series expansions and others that appear in this article is given in Appendix A, where (13) is taken as an example.

C. Resonance Conditions and Coupling for Lowest ESA Q

Of interest is the coupling between electric and magnetic modes, as these provide resonance at electrically small sizes. The resonant modal coupling transformer turns ratio $N = N_{pq}^{\mathrm{TE}}/N_{nm}^{\mathrm{TM}}$ in this case can be extracted by solving

$$X_{nm}^{\mathrm{TM}} + N^2 X_{pq}^{\mathrm{TE}} = 0 \tag{16}$$

for any coupled TM_{nm}–TE_{pq} system as follows:

$$N^2 = -\frac{(kaj_n)'(kay_n)'}{\left(kaj_p\right)\left(kay_p\right)}. \tag{17}$$

It can be shown numerically that this choice of modal coupling N not only provides resonance for any choice of ka, but also the lowest possible Q through a TM_{1m}–TE_{1q} system for sufficiently small ka, e.g., $ka \lessapprox 2$. The same analysis can be made for the coupling of two TM modes or two TE modes by modification of the resonance condition in (16); however, these modes may not resonate at electrically small sizes. Some choices of mode order and electrical size yield negative N^2 and, hence, imaginary N. If this result is obtained, it implies that the modes under consideration both have either capacitive or inductive input reactances at this electrical size and, hence, cannot be made to resonate. As would be expected, it can also be shown that the Laurent series expansion of (17) about $ka = 0$ for values $n = 1$ and $p = 1$ yields

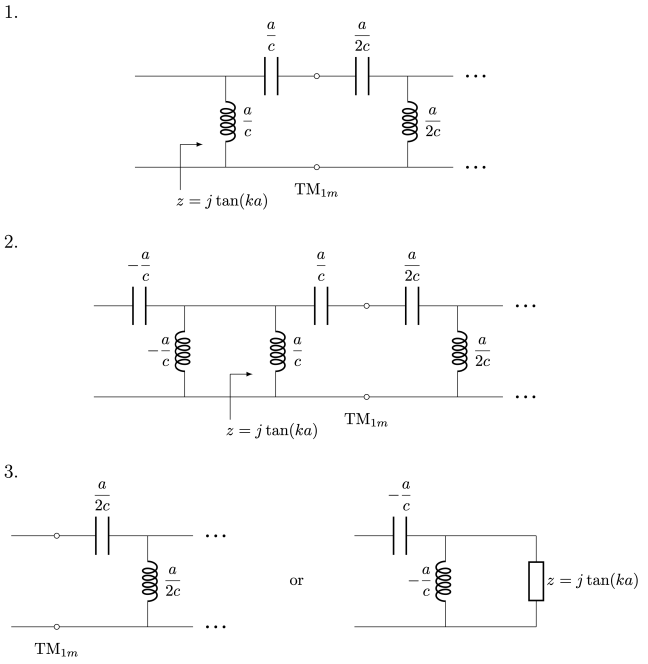

Fig. 4. Derivation for the equivalent TM_{1m} interior non-Foster circuit.

$$N^2 = \frac{2}{(ka)^2} + \mathcal{O}(1) \tag{18}$$

and for $n = 1$ and $p = 2$ yields

$$N^2 = \frac{10}{3(ka)^2} + \mathcal{O}(1) \tag{19}$$

as was shown by extreme truncation of the interior circuits, assuming small ka, by Thal [5]. By contrast, the newly derived equations are exact and valid for all ka.

III. Circuit-Based Derivation of Quality Factor and AR

A. Non-Foster Equivalent Circuits

The two-element methodology outlined in Section II is suitable to determine impedance quantities of the modes. However, to facilitate the calculation of other quantities, expansion of the Bessel-type loads into more traditional circuit elements proves useful. Along with the infinite ladder network for the internal fields, Thal [3] also provides "non-Foster" equivalent circuits (circuits using negative inductors and capacitors), though does not use them in determining analytical limits on Q. The process for obtaining these non-Foster equivalent circuits is shown pictorially in Fig. 4, with the TM_{1m} mode as an example. The resulting circuits for the TM_{1m} and TE_{1q} modes are shown in Fig. 5. It can be seen from the

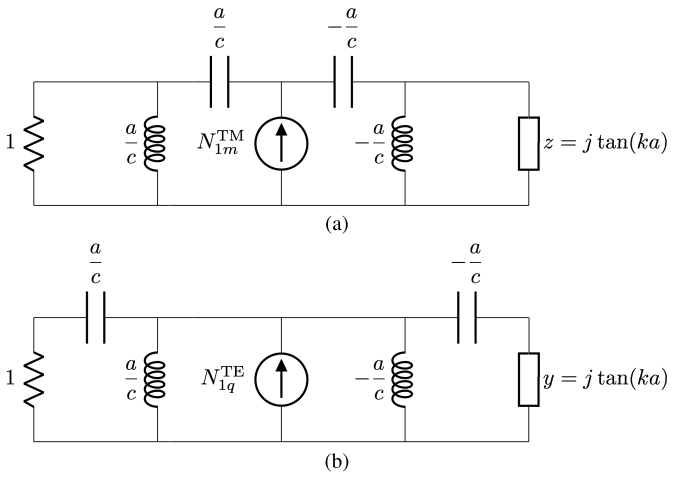

Fig. 5. Equivalent non-Foster representation of (a) TM_{1m} and (b) TE_{1q} modal circuits.

derivation and resulting circuits that to generate the non-Foster equivalent circuit, the interior circuit is the non-Foster image of the exterior circuit in Fig. 1. The interior circuit is then terminated in a impedance/admittance $j\tan(ka)$ (as opposed to a resistance), depending on which of the two circuits of Fig. 1 the mode corresponds to.

These circuits can be used to verify the results of Section II. As an example, the TM_{1m}–TE_{1q} system, the modal coupling quantity N^2, which yields resonance, can now be found from direct circuit analysis. The input reactances of both circuits are computed and combined in the same way as (16) to find N^2 as follows:

$$N^2 = \frac{2(ka)^3 - 2ka + \left[1 - 3(ka)^2 + (ka)^4\right]\tan(2ka)}{2(ka)^3 + \left[(ka)^4 - (ka)^2\right]\tan(2ka)} \tag{20}$$

which is the special case of (17) for $n = p = 1$, expressed using only elementary functions.

B. AR and Conditions for Circular Polarization

In applying the equivalent circuits of Fig. 5 to the modal coupling circuit, analytical expressions for the power delivered to the terminating resistance, and hence the far-field of each mode, can be derived via direct circuit analysis once said equivalent circuits are substituted into Fig. 2. The ratio of currents flowing through the TM_{1m} ($I_{1m,\mathrm{R}}^{\mathrm{TM}}$) and TE_{1q} ($I_{1q,\mathrm{R}}^{\mathrm{TE}}$) resistances can be found, including a phase term. This same phase term is also obtained when the modes are solved in isolation (i.e., not coupled via the transformer network) and combined. The currents running though the terminating resistor (of unity resistance) of each modal circuit when excited by a unit current are

$$I_{1m,\mathrm{R}}^{\mathrm{TM}} = je^{-jka}\cdot(kaj_1)' \tag{21}$$
$$I_{1q,\mathrm{R}}^{\mathrm{TE}} = -e^{-jka}\cdot(kaj_1) \tag{22}$$

where the constituent elementary functions have been reassembled as Bessel functions for purposes of comparison with previous results. It is seen that (8) and (9) (nonunity resistances excited by a unit current), and (21) and (22) (nonunity currents flowing through a unit resistance) suggest the same dissipated powers, with their different methods of analysis.

These results can then be applied to the coupled TM_{1m}–TE_{1q} circuit to derive the ratio

$$\frac{I_{1q,\mathrm{R}}^{\mathrm{TE}}}{I_{1m,\mathrm{R}}^{\mathrm{TM}}} = jN\cdot\frac{kaj_1}{(kaj_1)'} \tag{23}$$

where the TE mode current is scaled by the transformer using the turns ratio N. The current ratio of (23) implies that the modes under investigation always have quadrature phase as was shown, albeit only numerically, by Thal [5]. With analytical results for both phase and amplitude, the AR of a spherical wire antenna radiating only the TM_{1m} and TE_{1m} modes is

$$\mathrm{AR}^2 = \max\left(\frac{R_{1m}^{\mathrm{TM}}}{N^2R_{1m}^{\mathrm{TE}}}, \frac{N^2R_{1m}^{\mathrm{TE}}}{R_{1m}^{\mathrm{TM}}}\right). \tag{24}$$

This AR applies in all directions, as the modes under consideration have the same radiation pattern, though radiate in orthogonal and linear polarizations. This equation then specifies the modal coupling N for circular polarization of TM_{1m}–TE_{1m} radiators as follows:

$$N^2 = \frac{R_{1m}^{\mathrm{TM}}}{R_{1m}^{\mathrm{TE}}}. \tag{25}$$

When N is selected for resonance, the AR for electrically small TM_{1m}–TE_{1m} radiators is

$$\mathrm{AR}^2 = -\frac{(kaj_1)'(kay_1)}{(kaj_1)(kay_1)'} \tag{26}$$

which is the AR of the lowest Q TM_{1m}–TE_{1m} electrically small spherical wire antenna.

C. Stored Energy and Quality Factor

Using the circuits in Fig. 5, the exact stored energy of the modes can also be determined. While the majority of the circuit analysis needed to find the stored electric and magnetic energy is to find the currents through and voltages across inductors and capacitors, the stored energy in the impedance/admittance $j\tan(ka)$ is also required. Two equations from [14] of a lossless load of reactance X can be modified to fit into this problem

$$\frac{\omega W_{\mathrm{e}}}{|I|^2} = \frac{1}{8}\left(kaX' - X\right) \tag{27}$$
$$\frac{\omega W_{\mathrm{m}}}{|I|^2} = \frac{1}{8}\left(kaX' + X\right) \tag{28}$$

where unlike [14], the primes still indicate differentiation with respect to ka. It would be appealing to substitute (10) or (11) into (27) and (28) and obtain general equations for the stored energy of the modes, though this would be an approximation. Equations (27) and (28) apply only to reactances of *lossless* systems, and therefore, all uses of these equations herein are applied only to impedances with $\mathrm{Re}(Z) = 0$ to maintain an exact analysis. Noting this, the equations can be applied to the $j\tan(ka)$ loads to obtain

$$\frac{\omega W_{\mathrm{e}}(z = j\tan ka)}{|I|^2} = \frac{ka\csc^2 ka - \cot ka}{8} \tag{29}$$

TABLE I
COEFFICIENTS FOR THE STORED ENERGY EQUATIONS OF THE TM_{1m} AND TE_{1q} MODES

i	TM						TE					
	e			m			e			m		
	a_i	b_i	c_i	a_i	b_i	c_i	a_i	b_i	c_i	a_i	b_i	c_i
−4	0	0	−5	0	0	−3	0	0	0	0	0	0
−3	2	8	0	2	4	0	0	0	0	0	0	0
−2	0	0	9	0	0	3	0	0	−3	0	0	−1
−1	−2	−4	0	−2	0	0	2	4	0	2	0	0
0	0	0	−1	0	0	1	0	0	1	0	0	−1
1	2	0	0	2	0	0	2	0	0	2	0	0

$$\frac{\omega W_{\mathrm{m}}(z=j\tan ka)}{|I|^2}=\frac{ka\csc^2 ka+\cot ka}{8} \tag{30}$$

$$\frac{\omega W_{\mathrm{e}}(y=j\tan ka)}{|I|^2}=\frac{ka\sec^2 ka+\tan ka}{8} \tag{31}$$

$$\frac{\omega W_{\mathrm{m}}(y=j\tan ka)}{|I|^2}=\frac{ka\sec^2 ka-\tan ka}{8}. \tag{32}$$

With these, the stored energy of the modes can be determined via circuit analysis to derive equations of stored energy in terms of only elementary functions. It is possible to separate interior and exterior stored energy in this manner. For the purposes of later work in this article, the total stored energies of the TM_{1m} and TE_{1q} modes are derived and found to be

$$\frac{\omega W_{1m}}{|I|^2}=\frac{1}{16}\sum_{i=-4}^{1}(ka)^i[a_i+b_i\cos(2ka)+c_i\sin(2ka)] \tag{33}$$

with coefficients a_i, b_i, and c_i given in Table I. With the results obtained thus far, the Q of a coupled TM_{nm}–TE_{pq} system is then obtained analytically as follows:

$$Q=2\omega\frac{\max\left(W^{\mathrm{TM}}_{\mathrm{e},nm}+N^2W^{\mathrm{TE}}_{\mathrm{e},pq},\ W^{\mathrm{TM}}_{\mathrm{m},nm}+N^2W^{\mathrm{TE}}_{\mathrm{m},pq}\right)}{\frac{1}{2}R^{\mathrm{TM}}_{nm}+\frac{1}{2}N^2R^{\mathrm{TE}}_{pq}} \tag{34}$$

where the stored energies W are those of a unit current excitation.

While the above methodology is general and applies to all modes, solving a circuit for every mode may be impractical for a more general analysis. Thus, a general procedure is outlined below to generate stored energy equations, separating electric from magnetic energy, in the interior and exterior regions, for any order. The stored energy of a lossless interior region is simple to obtain; the equations

$$\frac{\omega W_{\mathrm{e}}}{|V|^2}=\frac{1}{8}\left(kaB'+B\right) \tag{35}$$

$$\frac{\omega W_{\mathrm{m}}}{|V|^2}=\frac{1}{8}\left(kaB'-B\right) \tag{36}$$

found in [14] for a lossless load of susceptance B can be used to obtain the stored energy from the inwardly directed wave impedances of (5) and (6) [via $B=\mathrm{Im}(1/Z)$] as follows:

$$\frac{\omega W^{\mathrm{TM}-}_{\mathrm{e},nm}}{|V^{\mathrm{TM}}_{nm}|^2}=\frac{ka\left[(kaj_n)'\right]^2-kaj_n\left[ka(kaj_n)''-(kaj_n)'\right]}{8\left[(kaj_n)'\right]^2} \tag{37}$$

$$\frac{\omega W^{\mathrm{TM}-}_{\mathrm{m},nm}}{|V^{\mathrm{TM}}_{nm}|^2}=\frac{ka\left[(kaj_n)'\right]^2-kaj_n\left[ka(kaj_n)''+(kaj_n)'\right]}{8\left[(kaj_n)'\right]^2} \tag{38}$$

$$\frac{\omega W^{\mathrm{TE}-}_{\mathrm{e},pq}}{|V^{\mathrm{TE}}_{pq}|^2}=\frac{ka\left[(kaj_n)'\right]^2-kaj_p\left[ka\left(kaj_p\right)''+\left(kaj_p\right)'\right]}{8\left(kaj_p\right)^2} \tag{39}$$

$$\frac{\omega W^{\mathrm{TE}-}_{\mathrm{m},pq}}{|V^{\mathrm{TE}}_{pq}|^2}=\frac{ka\left[(kaj_n)'\right]^2-kaj_p\left[ka\left(kaj_p\right)''-\left(kaj_p\right)'\right]}{8\left(kaj_p\right)^2} \tag{40}$$

where the voltages can be determined from the currents supplied to the mode as follows:

$$V^s_{nm}=\left(R^s_{nm}+jX^s_{nm}\right)I^s_{nm} \tag{41}$$

recalling that s represents either TM or TE. The choice to determine the stored energy in terms of applied voltage is chosen, as this voltage is the same for the interior and exterior networks. Similar to (27) and (28), (35) and (36) cannot be applied to lossy loads and, thus, cannot be used to compute the stored energy from the outwardly directed wave impedances of (3) and (4). Instead, a more general circuit approach is taken. The exterior circuits of Fig. 1 can be seen as a cascade of T or π networks, depending on if the mode is TM or TE—with some elements acting as perfect open or short circuits in the case of odd n (being reactances with zero inductance/capacitance). Given the relations between reactance values of the circuit, the currents and voltages at one port of these two-port sections are determined by those at the other port as follows:

$$\begin{bmatrix}V^s_{i-2}\\ I^{s+}_{i-2}\end{bmatrix}=\begin{bmatrix}A^s_i & B^s_i\\ C^s_i & D^s_i\end{bmatrix}\begin{bmatrix}V^s_i\\ I^{s+}_i\end{bmatrix} \tag{42}$$

where

$$A^{\mathrm{TM}}_i=D^{\mathrm{TE}}_i=\frac{(ka)^2-2i^2+3i-1}{(ka)^2} \tag{43}$$

$$B^{\mathrm{TM}}_i=C^{\mathrm{TE}}_i=j\frac{(2i-1)\left(i^2-i-(ka)^2\right)}{(ka)^3} \tag{44}$$

$$C^{\mathrm{TM}}_i=B^{\mathrm{TE}}_i=j\frac{1-2i}{ka} \tag{45}$$

$$D^{\mathrm{TM}}_i=A^{\mathrm{TE}}_i=\frac{(ka)^2-2i^2+i}{(ka)^2}. \tag{46}$$

The initial voltage, having the largest subscript value $i=n$ (n as usual being the mode order, to be replaced by p for TE modes), is the same voltage given in (41), with I^s_{nm} taken as unity. The initial currents are

$$I^{s+}_n=-\frac{V^s_{nm}}{Z^{s+}_{nm}} \tag{47}$$

where the sign of these currents is simply a matter of what direction they are defined to flow and Z_{nm}^{s+} is the impedance of (3) or (4). With the voltages and currents computed, the stored energies of the exterior region are

$$\frac{\omega W_{\mathrm{e},nm}^{\mathrm{TM}+}}{\left|I_{nm}^{\mathrm{TM}}\right|^2} = \sum_{\substack{i=1 \text{ or } 2 \\ i\equiv n \ (\mathrm{mod}\ 2)}}^{n} \frac{(i-1)\left|I_{i-2}^{\mathrm{TM}+}\right|^2 + i\left|I_{i}^{\mathrm{TM}+}\right|^2}{4ka} \tag{48}$$

$$\frac{\omega W_{\mathrm{m},nm}^{\mathrm{TM}+}}{\left|I_{nm}^{\mathrm{TM}}\right|^2} = \sum_{\substack{i=1 \text{ or } 2 \\ i\equiv n \ (\mathrm{mod}\ 2)}}^{n} \frac{ka\left|I_{i-2}^{\mathrm{TM}+} - I_{i}^{\mathrm{TM}+}\right|^2}{8i-4} \tag{49}$$

$$\frac{\omega W_{\mathrm{e},pq}^{\mathrm{TE}+}}{\left|I_{pq}^{\mathrm{TE}}\right|^2} = \sum_{\substack{i=1 \text{ or } 2 \\ i\equiv p \ (\mathrm{mod}\ 2)}}^{p} \frac{ka\left|V_{i-2}^{\mathrm{TE}} - V_{i}^{\mathrm{TE}}\right|^2}{8i-4} \tag{50}$$

$$\frac{\omega W_{\mathrm{m},pq}^{\mathrm{TE}+}}{\left|I_{pq}^{\mathrm{TE}}\right|^2} = \sum_{\substack{i=1 \text{ or } 2 \\ i\equiv p \ (\mathrm{mod}\ 2)}}^{p} \frac{(i-1)\left|V_{i-2}^{\mathrm{TE}}\right|^2 + i\left|V_{i}^{\mathrm{TE}}\right|^2}{4ka} \tag{51}$$

where $i \equiv n \ (\mathrm{mod}\ 2)$ indicates that i and n are always of the same parity (the sum is over only odd or even integers, depending in the parity of n), and likewise for $i \equiv p \ (\mathrm{mod}\ 2)$.

With the above equations determined, the Q of a general spherical wire antenna can be found, supporting a single mode or multiple modes. For a single mode, the Q is

$$Q_{nm}^{s} = 2\omega \frac{\max\left(W_{\mathrm{e},nm}^{s+} + W_{\mathrm{m},nm}^{s-},\ W_{\mathrm{m},nm}^{s+} + W_{\mathrm{m},nm}^{s-}\right)}{\frac{1}{2}R_{nm}^{s}} \tag{52}$$

where again a unit current excitation I_{nm}^{s} is assumed without loss of generality. For multiple modes, this Q is

$$Q = 2\omega \frac{\max\left(\sum_{n,m,s}\left(N_{nm}^{s}\right)^2 W_{\mathrm{e},mn}^{s},\ \sum_{n,m,s}\left(N_{nm}^{s}\right)^2 W_{\mathrm{m},mn}^{s}\right)}{\frac{1}{2}\sum_{n,m,s}\left(N_{nm}^{s}\right)^2 R_{mn}^{s}} \tag{53}$$

where I_{nm}^{s} is taken as unity for all modes (the relative modal excitation accounted for via inclusion of transformer turn ratios in the above equation)

$$W_{\mathrm{e},nm}^{s} = W_{\mathrm{e},nm}^{s+} + W_{\mathrm{e},nm}^{s-} \tag{54}$$

and

$$W_{\mathrm{m},nm}^{s} = W_{\mathrm{m},nm}^{s+} + W_{\mathrm{m},nm}^{s-}. \tag{55}$$

The only unknowns in (53) are the electrical size ka and transformer turns N_{nm}^{s}. The quantity N_{nm}^{s} can be obtained from (12), using the far-field radiation pattern by integrating over the far-field pattern and applying the orthogonality of the modes to obtain P_{nm}^{s}. Thus, the Q of a spherical wire antenna is fully defined by its electrical size and radiation pattern, if known exactly.

IV. Quality Factor and Polarization Purity Trade-Off

The exact relationship between the AR and Q on the electrical size ka and the modal coupling N has been demonstrated. It will now be shown analytically that the lowest Q TM_{1m}–TE_{1m} antenna has, in general, elliptical polarization,

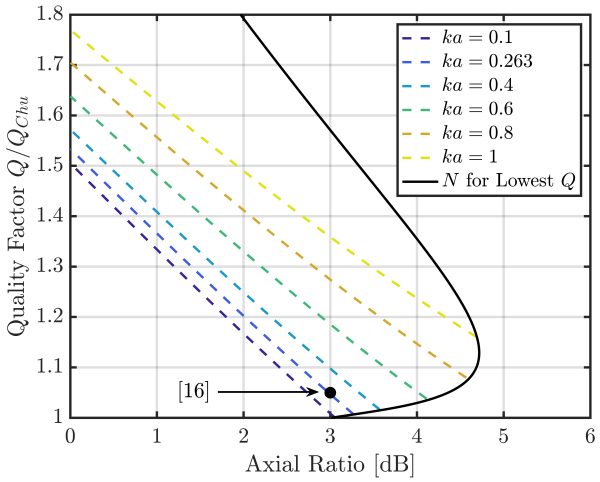

Fig. 6. Relationship between AR and Q. Colored lines: trade-off between Q and AR for various electrical sizes while varying N. Black line: AR with N selected for minimum Q while varying electrical size. Dot: elliptically polarized antenna of Best [16] included for reference.

whereas circular or linear polarization is usually preferred. First, circular polarization is analyzed, where the required compromise on Q for better polarization purity is demonstrated. With both the AR and Q determined by ka and N, their relationship can be evaluated quantitatively. A first look is given in Fig. 6, where Q and AR are the axes, while N is left to vary for constant ka, or vice versa. In effect, this plot states the lower bound on Q for a required AR and electrical size. An elliptically polarized spherical wire antenna ($ka \approx 0.263$) proposed by Best [16] is annotated on the plot. As can be seen, Best [16] achieved nearly the best possible Q (61.7) for the reported AR of 3 dB and the antenna's electrical size. The contents of the plot are well summarized by considering the Laurent series expansion of Q in terms of ka, with coefficients dependent on AR

$$Q_{\mathrm{NCP}} = \frac{1}{\mathrm{AR}^2+1}\left(\frac{3}{(ka)^3} + \frac{3+21\mathrm{AR}^2/20}{ka}\right) + \mathcal{O}(ka) \tag{56}$$

which applies for "near-circular polarization" having AR more circularly polarized than (26), the AR of a resonant antenna. By the nature of its derivation, (56) is increasingly accurate for smaller ka. Equation (56) is, thus, a convenient shorthand for computing the required compromise on circularly polarized ESA Q for improved AR. It is clear from the form of the equation that the $1/(ka)$ term can be discarded for $ka \ll 1$.

Equation (25) can be used to determine the modal coupling N, which achieves circular polarization, a known deviation from the ideal modal coupling, which provides minimum Q. The resulting Q can then be computed with (34). Similarly, linear or lowest Q elliptical polarization can be analyzed by the choice of N outlined above. A plot of the smallest Q air-core spherical wire antenna, which provides various polarizations, is shown in Fig. 7. It can be seen that both linearly and circularly polarized antenna Q curves converge to $1.5Q_{\mathrm{Chu}}$ as $ka \to 0$. Notably, this comparison implies that while elliptical polarization yields the lowest Q, of the polarizations considered "pure", linear polarization—and not

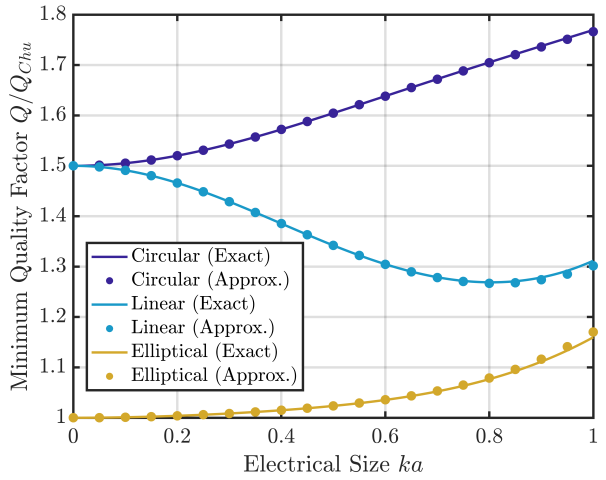

Fig. 7. Minimum Q for a TM_{1m}–TE_{1m} spherical wire antenna for various polarizations. Approximations are taken ignoring Laurent series terms $\mathcal{O}[(ka)^5]$ and higher.

circular polarization—yields the lowest Q of an electrically small spherical wire antenna. For convenience, Laurent series approximations for the Q of circularly polarized (Q_{CP}), linearly polarized (Q_{LP}), and elliptically polarized (Q_{EP}) lower bounds are provided, valid for small ka, and are compared against the exact expressions in Fig. 7

$$Q_{\mathrm{LP}} = \frac{3}{2(ka)^3} + \frac{3}{5ka} + \frac{587ka}{1400} + \frac{757(ka)^3}{9000} + \mathcal{O}\left[(ka)^5\right] \quad (57)$$

$$Q_{\mathrm{CP}} = \frac{3}{2(ka)^3} + \frac{81}{40ka} - \frac{11ka}{700} + \frac{1157(ka)^3}{50400} + \mathcal{O}\left[(ka)^5\right] \quad (58)$$

$$Q_{\mathrm{EP}} = \frac{1}{(ka)^3} + \frac{11}{10ka} + \frac{11ka}{700} + \frac{14141(ka)^3}{63000} + \mathcal{O}\left[(ka)^5\right]. \quad (59)$$

Note that the limiting form of (59) agrees with the result obtained in [13] for the self-tuned, free-space, electric-current spherical dipole antenna.

By substituting AR $=1$ into (56), the first two terms of (58) are recovered. Equation (57), being the Q of the TM_{1m} modes, is similar to that of Hansen and Collin [17] who obtain their expression by a curve fitting procedure (and, thus, their expression contains floating point numbers rather than exact fractions). In contrast, the Laurent series approach taken here suggests higher order terms, which provide improved accuracy for larger ka values, and a prescription for how to obtain higher order terms for accuracy at larger ka should it be required. From the above analysis, it is clear why Hansen and Collin [17] had difficulty fitting to the curve $Q = A/(ka) + B/(ka)^2 + C/(ka)^3$, since even order terms are not present in the above expansions. From the decimals obtained from curve fitting, Hansen and Collin [17] suggest an alternative approximation with irrational coefficients, though the above has shown no irrational numbers are present in the lowest order terms. In both cases, agreement is seen that the lowest order term is $3/[2(ka)^3]$.

V. Comparison With Field Integration Method

With exact equations for Q of the circuits of Thal [5] determined, agreement between circuit and field perspectives is readily examined. Collin and Rothschild [2] suggest that their field integration-based Q values are the same as those for Chu's circuits (when the circuits are solved exactly) for the $n \in \{1, 2, 3\}$ modes, though they did not verify any higher order modes on account of the algebraic complexity of the problem. Both calculations consider stored energy only external to the Chu sphere, and the Collin and Rothschild analysis did not consider coupled modes. Fante [8] then provided expressions for Q considering both electric and magnetic energies external to the Chu sphere, allowing for coupled-mode Q calculation from field integration, and quantified the difference between his equations against the approximate expressions for Q provided by Chu [1]. In Fante's work, agreement is only shown for small ka. McLean [4] then found that when the circuits are solved exactly for $n = 1$, the *coupled* combinations of the TM_{1m} and TE_{1q} modes agree with Fante [8], as well as with Collin and Rothschild [2] for all ka. To date, the circuit and field integration formalisms have been shown to agree only to this very limited extent. What remained to be shown was that the general nth-order network of Chu (when solved exactly) and the field integration techniques agreed in general. One factor constraining this discovery was the fact that *exact* solutions to Chu's circuits for the nth-order circuit were not available. Later, Thal [5] generalized Chu's circuits to account for energy both interior and exterior to the Chu sphere of a spherical wire antenna, while Hansen et al. [9] performed the same generalizations using the field integration techniques. In this section, the agreement of the circuit and field formalisms will be shown in *all* cases of electric current excitation by way of comparing the equations derived herein (based on the networks of Thal [3]) with Hansen et al. [9], which both account for stored energy exterior and interior of the Chu sphere and present exact equations for *arbitrary* mode order and electrical size.

To make this comparison, a subset of Q's are defined. In all cases, the Q definitions are the usual

$$Q = \frac{2\omega W}{P}. \quad (60)$$

An *external* Q (which will be denoted with a superscript $+$) is where W is taken as the energy exterior to the Chu sphere, whereas an *internal* Q (denoted with superscript $-$) is where W is taken as the energy interior to the Chu sphere. Similarly, an electric Q (with roman/upright subscript e) is where W is taken as the electric energy only, regardless of whether it is the larger of the electric or magnetic energies. Similarly, a magnetic Q (with roman/upright subscript m) is that where W is the magnetic energy only. The power P is the same radiated power in all cases. These qualifiers can be combined and associated with a mode, e.g., external electric TM_{1m} Q denoted as $Q^{\mathrm{TM}+}_{\mathrm{e},1m}$, which is the Q of (1). With these subdivisions, the total Q of a mode is then

$$Q^s_{nm} = \max\left\{Q^{s+}_{\mathrm{e},nm} + Q^{s-}_{\mathrm{e},nm},\ Q^{s+}_{\mathrm{m},nm} + Q^{s-}_{\mathrm{m},nm}\right\}. \quad (61)$$

The utility in this subdivision is that all four permutations of external, internal, electric, and magnetic can be compared separately to establish complete agreement in Q predictions between the circuit and field integration approaches. Similar subsets are defined in [8] and [9], notated with primes.

For the claims of equality that follow, overviews for the proofs are given in Appendix B. The equations of this article and those of [9] show that *internal* Q values of both circuit and field integration formalisms are identical for all mode orders n, for all ka, and for both TM and TE modes. This verification is performed by simply equating the expressions for Q^- of the two formalisms, which are then manipulated to show the equality is true. This was verified analytically for the general nth-order case. The external Q requires a more sophisticated argument, owing to the forms derived from the circuit formalism. The external Q is shown to agree between circuit and field integration formalisms via an argument from mathematical induction. For modes $n \in \{1, 2\}$, the external electric and magnetic Q values are found analytically equivalent between the two formalisms—for both TM and TE modes—in the same manner as the internal Q^- expressions. This can be verified by simply expanding the sums for externally stored energy, incorporating them into a measure of Q, and then showing equality with similar expressions derived from [9]. These $n \in \{1, 2\}$ serve as the base case for the inductive argument. Next, recurrence relations can be derived from the circuit formalism, relating the Q^+ of mode order n mode to that of mode order $n + 2$. The relations are

$$Q^{\mathrm{TM}+}_{\mathrm{e},n+2,m} = Q^{\mathrm{TM}+}_{\mathrm{e},nm} + \frac{4}{R^{\mathrm{TM}}_{nm}} \cdot \frac{(n+1)\left|I^{\mathrm{TM}+}_{n}\right|^2 + (n+2)\left|I^{\mathrm{TM}+}_{n+2}\right|^2}{4ka} \tag{62}$$

$$Q^{\mathrm{TM}+}_{\mathrm{m},n+2,m} = Q^{\mathrm{TM}+}_{\mathrm{m},nm} + \frac{4}{R^{\mathrm{TM}}_{nm}} \cdot \frac{ka\left|I^{\mathrm{TM}+}_{n} - I^{\mathrm{TM}+}_{n+2}\right|^2}{8n+12} \tag{63}$$

$$Q^{\mathrm{TE}+}_{\mathrm{e},p+2,q} = Q^{\mathrm{TE}+}_{\mathrm{e},pq} + \frac{4}{R^{\mathrm{TE}}_{pq}} \cdot \frac{ka\left|V^{\mathrm{TE}}_{p} - V^{\mathrm{TE}}_{p+2}\right|^2}{8p+12} \tag{64}$$

$$Q^{\mathrm{TE}+}_{\mathrm{m},p+2,q} = Q^{\mathrm{TE}+}_{\mathrm{m},pq} + \frac{4}{R^{\mathrm{TE}}_{pq}} \cdot \frac{(p+1)\left|V^{\mathrm{TE}}_{p}\right|^2 + (p+2)\left|V^{\mathrm{TE}}_{p+2}\right|^2}{4ka} \tag{65}$$

where the additional currents and voltages are found from

$$\begin{bmatrix} V^s_{n+2} \\ I^{s+}_{n+2} \end{bmatrix} = \begin{bmatrix} A^s_{n+2} & B^s_{n+2} \\ C^s_{n+2} & D^s_{n+2} \end{bmatrix}^{-1} \begin{bmatrix} V^s_n \\ I^{s+}_n \end{bmatrix} \tag{66}$$

and V^s_n and I^{s+}_n are the voltage and current used to produce Q_{nm}, all assuming (without loss of generality) a mode excitation I^s_{nm} of unity.

It is found that all external Q^+ of this work and equivalent formulations of these Q^+ from the externally stored energies and radiated powers of [9] obey these recurrence relations for arbitrary mode order. Thus, since all external Q^+ equations between this work and that of [9] agree for the cases $n \in \{1, 2\}$, and both formalisms relate the mode order $n + 2$ to the mode order n in exactly the same way, they are shown to be equivalent for all n via a proof by mathematical induction. Therefore, the circuit work of Thal [5] and the field integration work of Hansen et al. [9] have been shown to make the exact same predictions of Q for arbitrary multipoles, at arbitrary electrical sizes, accounting for electric currents, which excite stored electric and magnetic energy both inside and outside of a spherical wire antenna. Furthermore, it can then be inferred that the bases for these works—circuits derived from modal wave impedances (Chu [1]), and field integration with subtraction of the far fields (Collin and Rothschild [2] and Fante [8])—produce the exact same predictions in all cases of electric current excitation. Previous work by McLean [4] and Fante [8] demonstrates equality between circuit and field integration formalisms for special cases of low-order modes, only accounting for energy external to the Chu sphere. This work then generalizes the unity of these formalisms to all multipoles, accounting for fields interior and exterior to the Chu sphere, without any assumption on electrical size ka. While special case agreement is not atypical for many other Q calculations of antennas (e.g., agreement at small ka), it is now clear that these two methods of computing Q are completely equivalent (at least for the class of air-filled spherical wire antennas carrying electric currents).

VI. Conclusion

Exact properties of air-core spherical wire antennas have been revisited from the circuit perspective. It is shown that the circuit analysis approach to the study of ESAs via spherical waves is in agreement with the field integration perspective for arbitrary multipoles. The Q predictions concerning stored energy of the interior region of a spherical wire antenna from circuit and field integration formalisms are compared to show direct equality in the nth-order case, while an argument from mathematical induction is used for Q predictions concerning the energies stored in the exterior of a spherical wire antenna. Furthermore, the presented analytical circuit approach established exact equations for the radiated power, resonance conditions of coupled-mode systems, and quantitative demonstrations of the trade-off of quality factor and polarization purity. Some Laurent expansions are taken to show these new results to be the general cases of previous work, while other Laurent expansions provide new and simple equations to quantify the limits of small antennas, for use when the exact Bessel-related expressions prove to be superfluous.

Appendix A
Sample Computation of Bessel Function-Related Laurent Series Expansions

This appendix serves as a guide for the computation of Laurent series expansions involving spherical Bessel functions, as they appear in the main body of this article. Derivation of (13) is taken as an example, though other Laurent series' can be obtained via a similar procedure. Spherical Bessel functions of the second kind can be converted to those of the first kind as $y_n = (-1)^{n+1} j_{-n-1}$, which is convenient so as to use only one Bessel-related power series. Starting with

$$X^{\mathrm{TM}}_{10} = -(kaj_1)'(kay_1)' = -(kaj_1)'(kaj_{-2})' \tag{A.1}$$

the product rule can be used to obtain

$$X^{\mathrm{TM}}_{10} = -\left[j_1 j_{-2} + kaj_1 j_{-2} + kaj'_1 j'_{-2} + (ka)^2 j'_1 j'_{-2}\right]. \tag{A.2}$$

Hereafter, a known series expansion of the spherical Bessel function of the first kind is applied [18]

$$j_n = \sum_{i=0}^{\infty} \frac{\left(-\frac{1}{2}\right)^i (ka)^{2i+n}}{i!(2n+2i+1)!!} \tag{A.3}$$

and its derivative

$$j_n' = \sum_{i=0}^{\infty} \frac{(2i+n)\left(-\frac{1}{2}\right)^i (ka)^{2i+n-1}}{i!(2n+2i+1)!!} \tag{A.4}$$

to obtain expansions of the functions in (A.2). Only the first terms of each expansion are required to determine the $(ka)^{-1}$ term of the Laurent series expansion of (A.1), as determined a posteriori. These required terms are

$$j_1 = \frac{ka}{3} + \mathcal{O}\left[(ka)^3\right] \tag{A.5}$$

$$j_1' = \frac{1}{3} + \mathcal{O}\left[(ka)^2\right] \tag{A.6}$$

$$j_{-2} = -\frac{1}{(ka)^2} + \mathcal{O}(1) \tag{A.7}$$

$$j_{-2}' = \frac{2}{(ka)^3} + \mathcal{O}\left[(ka)^{-1}\right]. \tag{A.8}$$

Upon substituting these truncated expansions into (A.2), the TM_{10} input reactance is found to have the Laurent series expansion of

$$X_{10}^{\mathrm{TM}} = -\frac{2}{3ka} + \mathcal{O}(ka). \tag{A.9}$$

Other Laurent series expansions in this article can be found by a similar procedure. In cases involving trigonometric functions, their known Taylor or Laurent series expansions are to be employed (e.g., as tabulated in [18]). The only remaining complication is when spherical Bessel functions appear in the denominator of an expression to be expanded. In this case, the required series expansion is obtained from polynomial long division, starting with the lowest order terms of (A.3) or (A.4) (division by increasing powers). While, for an exact result, the division contains infinitely many steps, a truncated expression can be obtained, which is sufficient for the Laurent series exercise to which it is to be applied. Some pertinent examples are provided for reference, to high order of ka

$$\frac{1}{j_1} = \frac{3}{ka} + \frac{3ka}{10} + \frac{27(ka)^3}{1400} + \frac{19(ka)^5}{18000} + \mathcal{O}\left[(ka)^7\right] \tag{A.10}$$

$$\frac{1}{j_1'} = 3 + \frac{9(ka)^2}{10} + \frac{303(ka)^4}{1400} + \mathcal{O}\left[(ka)^6\right] \tag{A.11}$$

$$\frac{1}{j_{-2}} = -(ka)^2 + \frac{(ka)^4}{2} - \frac{3(ka)^6}{8} + \mathcal{O}\left[(ka)^8\right] \tag{A.12}$$

$$\frac{1}{j_{-2}'} = \frac{(ka)^3}{2} - \frac{(ka)^7}{16} + \frac{(ka)^9}{144} + \mathcal{O}\left[(ka)^{11}\right]. \tag{A.13}$$

Series expansions of reciprocals of sums of spherical Bessel functions can be obtained in a similar manner. Alternately, polynomial long division of increasing powers can be performed directly after all functions are replaced with their series expansions.

Appendix B
Proof Outline of Equality Between Circuit and Field Integration Quantities

A. Appendix Overview

For the proof of equality between the circuit and field integration formalisms, three results need to be proved: equality between formalisms of the internal Q_{nm}^{s-}, equality between formalisms of the base cases Q_{1m}^{s+} and Q_{2m}^{s+}, as well as showing both formalisms obey the recurrence relations in (62)–(65). For each of these, four permutations (electric/magnetic TM and electric/magnetic TE) need to be shown. However, between these four permutations, the proofs are quite similar; therefore, for brevity, only the electric TM case will be shown here.

B. Internal Quality Factor

The quantity $Q_{\mathrm{e},nm}^{\mathrm{TM}-}$ as derived herein is

$$Q_{\mathrm{e},nm}^{\mathrm{TM}-} = \frac{\omega W_{\mathrm{e},nm}^{\mathrm{TM}-}}{\left|V_{nm}^{\mathrm{TM}}\right|^2} \cdot \frac{4\left|R_{nm}^{\mathrm{TM}} + jX_{nm}^{\mathrm{TM}}\right|^2}{R_{nm}^{\mathrm{TM}}} \tag{B.1}$$

which can be expanded to

$$Q_{\mathrm{e},nm}^{\mathrm{TM}-} = \frac{ka\left[(kaj_n)'\right]^2 - kaj_n\left[ka(kaj_n)'' - (kaj_n)'\right]}{8\left[(kaj_n)'\right]^2} \cdot 4\left\{\left[(kaj_n)'\right]^2 + \left[(kay_n)'\right]^2\right\}. \tag{B.2}$$

The equivalent quantity from [9], denoted $\mathcal{Q}_{\mathrm{e},nm}^{\mathrm{TM}-}$, is

$$\mathcal{Q}_{\mathrm{e},nm}^{\mathrm{TM}-} = \frac{\left|\left(kah_n^{(1)}\right)'\right|^2}{\left[(kaj_n)'\right]^2}\left[\frac{(ka)^3}{2}\left(j_{n-1}^2 - j_{n-2}j_n\right) - nkaj_n^2\right]. \tag{B.3}$$

Since

$$\frac{\left|\left(kah_n^{(1)}\right)'\right|^2}{\left[(kaj_n)'\right]^2} = \frac{\left[(kaj_n)'\right]^2 + \left[(kay_n)'\right]^2}{\left[(kaj_n)'\right]^2} \tag{B.4}$$

upon assuming $Q_{\mathrm{e},nm}^{\mathrm{TM}-} = \mathcal{Q}_{\mathrm{e},nm}^{\mathrm{TM}-}$, these terms cancel from their respective sides to obtain

$$ka\left[(kaj_n)'\right]^2 - kaj_n\left[ka(kaj_n)'' - (kaj_n)'\right] = (ka)^3\left(j_{n-1}^2 - j_{n-2}j_n\right) - 2nkaj_n^2. \tag{B.5}$$

Expanding the derivates using standard identities and rearranging the left-hand side give

$$(ka)^3 j_{n-1}^2 - j_n^2\left[2nka - (ka)^3\right] - (ka)^2(2n-1)j_{n-1}j_n = (ka)^3\left(j_{n-1}^2 - j_{n-2}j_n\right) - 2nkaj_n^2 \tag{B.6}$$

which is readily shown true with the recurrence relation

$$j_{n-1} + j_{n+1} = \frac{2n+1}{ka} j_n. \tag{B.7}$$

C. Base Case for External Quality Factor

In this section, the $n = \{1, 2\}$ case is shown. The quantity $Q_{\mathrm{e},nm}^{\mathrm{TM}+}$ as derived herein is

$$Q_{\mathrm{e},nm}^{\mathrm{TM}+} = \frac{4\omega W_{\mathrm{e},nm}^{\mathrm{TM}+}}{\left|I_{nm}^{\mathrm{TM}}\right|^2 R_{nm}^{\mathrm{TM}}}. \tag{B.8}$$

The field integration expression from [9] is

$$\mathcal{Q}_{\mathrm{e},nm}^{\mathrm{TM}+} = ka + nka\left|h_n^{(1)}\right|^2 - \frac{(ka)^3}{2}\left[\left|h_{n-1}^{(1)}\right|^2 - \mathrm{Re}\left\{h_{n-2}^{(1)*}h_n^{(1)}\right\}\right]. \tag{B.9}$$

$$\mathcal{Q}^{\mathrm{TM}+}_{\mathrm{e},n+2,m} - \mathcal{Q}^{\mathrm{TM}+}_{\mathrm{e},nm} = \frac{2n+3}{(ka)^3}\Big\{\big|h_n^{(1)}\big|^2\big[(ka)^2\big((ka)^2 - 2(n+2)(2n+1)\big) + (n+2)(2n+3)(2n+1)^2\big] + (ka)^2\big|h_{n-1}^{(1)}\big|^2(n+2)(2n+3) + 2ka\cdot\mathrm{Re}\Big\{h_{n-1}^{(1)*}h_n^{(1)}\Big\}\big[(ka)^2 - (2n+3)(2n+1)\big](n+2)\Big\} \tag{B.18}$$

From (8) and (48), $\mathcal{Q}^{\mathrm{TM}+}_{\mathrm{e},1m}$ is

$$\mathcal{Q}^{\mathrm{TM}+}_{\mathrm{e},1m} = ka\big|h_1^{(2)}\big|^2 = \frac{1}{(ka)^3} + \frac{1}{ka} \tag{B.10}$$

as expected. The quantity $\mathcal{Q}^{\mathrm{TM}+}_{\mathrm{e},1m}$ is readily found evaluate to the same result with the simplification

$$\big|h_0^{(1)}\big|^2 - \mathrm{Re}\Big\{h_{-1}^{(1)*}h_1^{(1)}\Big\} = \frac{2}{(ka)^2} \tag{B.11}$$

recognizing that $|h_n^{(1)}| = |h_n^{(2)}|$. The $n = 2$ case is better handled by invoking trigonometric/exponential representations of spherical Bessel functions after simplifying as much as possible, since their order is known. After further manipulation, it can be shown that

$$\mathcal{Q}^{\mathrm{TM}+}_{\mathrm{e},2m} = \mathcal{Q}^{\mathrm{TM}+}_{\mathrm{e},2m} = \frac{18}{(ka)^5} + \frac{6}{(ka)^3} + \frac{3}{ka} \tag{B.12}$$

which is consistent with [2].

D. Induction Step for External Quality Factor

Expanding the stored energy in (B.8) gives

$$Q^{\mathrm{TM}+}_{\mathrm{e},nm} = \frac{4}{R^{\mathrm{TM}}_{nm}} \sum_{\substack{i=1 \text{ or } 2 \\ i\equiv n \,(\mathrm{mod}\,2)}}^{n} \frac{(i-1)\big|I^{\mathrm{TM}+}_{i-2}\big|^2 + i\big|I^{\mathrm{TM}+}_{i}\big|^2}{4ka} \tag{B.13}$$

where as usual, $Q^{\mathrm{TM}+}_{\mathrm{e},nm} = 2\omega W^{\mathrm{TM}+}_{\mathrm{e},nm}/P^{\mathrm{TM}}_{nm}$. Let the input current to this mode be unity, without loss of generality. Now, increasing the mode order by 2 involves simply appending a lossless high-pass T network to the input of the mode under investigation (a π network for the TE case). The voltages and currents can simply be solved in reverse, assuming a larger input current, which maintains the unit current at the branch, which was the input to the nth-order mode. This is the role of the matrix equation (66). Crucially, the radiated power in this case remains unchanged, as the additional T network is lossless; therefore, $P^{\mathrm{TM}}_{n+2,m} = P^{\mathrm{TM}}_{nm} = (1/2)R^{\mathrm{TM}}_{nm}$ for this analysis. The stored electric energy (multiplied by angular frequency) of the additional T network is

$$\omega\big(W^{\mathrm{TM}+}_{\mathrm{e},n+2,m} - W^{\mathrm{TM}+}_{\mathrm{e},nm}\big) = \frac{(n+1)\big|I^{\mathrm{TM}+}_{n}\big|^2 + (n+2)\big|I^{\mathrm{TM}+}_{n+2}\big|^2}{4ka}. \tag{B.14}$$

Since under the proposed current excitations

$$\frac{2\omega W^{\mathrm{TM}+}_{\mathrm{e},n+2,m}}{P^{\mathrm{TM}}_{n+2,m}} = \frac{2\omega W^{\mathrm{TM}+}_{\mathrm{e},nm}}{P^{\mathrm{TM}}_{nm}} + \frac{2\omega\big(W^{\mathrm{TM}+}_{\mathrm{e},n+2,m} - W^{\mathrm{TM}+}_{\mathrm{e},nm}\big)}{P^{\mathrm{TM}}_{nm}} \tag{B.15}$$

it is clear that

$$\mathcal{Q}^{\mathrm{TM}+}_{\mathrm{e},n+2,m} = \mathcal{Q}^{\mathrm{TM}+}_{\mathrm{e},nm} + \frac{4}{R^{\mathrm{TM}}_{nm}}\cdot\frac{(n+1)\big|I^{\mathrm{TM}+}_{n}\big|^2 + (n+2)\big|I^{\mathrm{TM}+}_{n+2}\big|^2}{4ka} \tag{B.16}$$

follows directly from the external TM circuits. After considerable manipulation, it can be shown that

$$\mathcal{Q}^{\mathrm{TM}+}_{\mathrm{e},n+2,m} = \mathcal{Q}^{\mathrm{TM}+}_{\mathrm{e},nm} + \frac{4}{R^{\mathrm{TM}}_{nm}}\cdot\frac{(n+1)\big|I^{\mathrm{TM}+}_{n}\big|^2 + (n+2)\big|I^{\mathrm{TM}+}_{n+2}\big|^2}{4ka} \tag{B.17}$$

can be expanded to (B.18), as shown at the top of the page, and shown to be true.

ACKNOWLEDGMENT

The authors thank the anonymous reviewers for identifying the potential of this work in establishing agreement between the circuit- and field-integration-based approaches and whose comments motivated a more thorough treatment of this agreement as detailed in Section V.

REFERENCES

[1] L. J. Chu, "Physical limitations of omni-directional antennas," *J. Appl. Phys.*, vol. 19, no. 12, pp. 1163–1175, Dec. 1948.
[2] R. E. Collin and S. Rothschild, "Evaluation of antenna Q," *IEEE Trans. Antennas Propag.*, vol. AP-12, no. 1, pp. 23–27, Jan. 1964.
[3] H. L. Thal, Jr., "Exact circuit analysis of spherical waves," *IEEE Trans. Antennas Propag.*, vol. 26, no. 2, pp. 282–287, Mar. 1978.
[4] J. S. McLean, "A re-examination of the fundamental limits on the radiation Q of electrically small antennas," *IEEE Trans. Antennas Propag.*, vol. 44, no. 5, pp. 672–676, May 1996.
[5] H. L. Thal, Jr., "New radiation Q limits for spherical wire antennas," *IEEE Trans. Antennas Propag.*, vol. 54, no. 10, pp. 2757–2763, Oct. 2006.
[6] H. L. Thal, Jr., "Gain and Q bounds for coupled TM-TE modes," *IEEE Trans. Antennas Propag.*, vol. 57, no. 7, pp. 1879–1885, Jul. 2009.
[7] C. Pfeiffer, "Fundamental efficiency limits for small metallic antennas," *IEEE Trans. Antennas Propag.*, vol. 65, no. 4, pp. 1642–1650, Apr. 2017.
[8] R. L. Fante, "Quality factor of general ideal antennas," *IEEE Trans. Antennas Propag.*, vol. AP-17, no. 2, pp. 151–155, Mar. 1969.
[9] T. V. Hansen, O. S. Kim, and O. Breinbjerg, "Stored energy and quality factor of spherical wave functions–in relation to spherical antennas with material cores," *IEEE Trans. Antennas Propag.*, vol. 60, no. 3, pp. 1281–1290, Mar. 2012.
[10] A. D. Yaghjian and S. R. Best, "Impedance, bandwidth, and Q of antennas," *IEEE Trans. Antennas Propag.*, vol. 53, no. 4, pp. 1298–1324, Apr. 2005.
[11] A. D. Yaghjian, "Overcoming the Chu lower bound on antenna Q with highly dispersive lossy material," *IET Microw., Antennas Propag.*, vol. 12, no. 4, pp. 459–466, Mar. 2018.
[12] M. Gustafsson, C. Sohl, and G. Kristensson, "Physical limitations on antennas of arbitrary shape," *Proc. Roy. Soc. A*, vol. 463, pp. 2589–2607, Oct. 2007.
[13] A. D. Yaghjian, M. Gustafsson, and B. L. G. Jonsson, "Minimum Q for lossy and lossless electrically small dipole antennas," *Prog. Electromagn. Res.*, vol. 143, pp. 641–673, 2013.
[14] R. F. Harrington, *Time-Harmonic Electromagnetic Fields*. New York, NY, USA: IEEE Press, 2001.
[15] D. A. Garren, "Radiation properties of pure magnetic dipole antenna with spherical current density via exact Maxwell solution," *IEEE Trans. Antennas Propag.*, vol. 70, no. 5, pp. 3469–3476, May 2022.
[16] S. R. Best, "Low Q electrically small linear and elliptical polarized spherical dipole antennas," *IEEE Trans. Antennas Propag.*, vol. 53, no. 3, pp. 1047–1053, Mar. 2005.

[17] R. C. Hansen and R. E. Collin, "A new Chu formula for Q," *IEEE Antennas Propag. Mag.*, vol. 51, no. 5, pp. 38–41, Oct. 2009.

[18] F. W. J. Olver, D. W. Lozier, R. F. Boisvert, and C. W. Clark, *The NIST Handbook of Mathematical Functions*. New York, NY, USA: Cambridge Univ. Press, 2010.

Alexander B. Murray (Graduate Student Member, IEEE) received the B.Sc. degree (Hons.) in electrical engineering from the University of Alberta, Edmonton, AB, Canada, in 2022, where he is currently pursuing the Ph.D. degree in electrical engineering.

He has been an undergraduate student researcher in the areas of harmonic radar, infrared fiber amplifiers, nuclear magnetic resonance, and folded dipole antennas. His current research interests include theoretical limitations on electrically small antennas and their design.

Mr. Murray has been a member of the IEEE Antennas and Propagation Society since 2022. He was a recipient of the Natural Sciences and Engineering Research Council (NSERC) of Canada Graduate Scholarship (Master's Level) in 2022 and, in 2023, was a recipient of the IEEE AP-S Eugene F. Knott Memorial Pre-Doctoral Research Grant and the IEEE AP-S Fellowship. He was also a member of a finalist student group in the 2022 APS/URSI Symposium Student Design Contest in Denver, CO, USA, which featured designs on the topic of miniaturized antenna of the Internet-of-Things (IoT) applications.

Ashwin K. Iyer (Senior Member, IEEE) received the B.A.Sc. (Hons.), M.A.Sc., and Ph.D. degrees in electrical engineering from the University of Toronto, Toronto, ON, Canada, in 2001, 2003, and 2009, respectively, with a focus on the discovery and development of the negative-refractive-index transmission-line approach to metamaterial design and the realization of metamaterial lenses for free-space microwave subdiffraction imaging.

He is currently a Professor and an Associate Dean, master's studies with the Department of Electrical and Computer Engineering, University of Alberta, Edmonton, AB, Canada, and the Director of the Microwave, Millimetre-Wave, and MetaDevices (M3) Laboratory. His research group investigates novel RF/microwave circuits and techniques, fundamental electromagnetic theory, antennas, sensors, and engineered metamaterials, with an emphasis on their applications to microwave and optical devices, defence technologies, and biomedicine. He has coauthored a number of highly cited papers and book chapters on the subject of metamaterials.

Dr. Iyer is a member of the IEEE AP-S AdCom, the Education Committee, the Membership and Benefits Committee, and the Young Professionals Committee. He was a recipient of the IEEE AP-S R. W. P. King Award in 2008, the IEEE AP-S Donald G. Dudley Jr. Undergraduate Teaching Award in 2015, the University of Alberta Provost's Award for Early Achievement of Excellence in Undergraduate Teaching in 2014, and the University of Alberta Rutherford Award for Excellence in Undergraduate Teaching in 2018. His students are the recipients of several major national and international awards for their research. He served as the Technical Program Committee Co-Chair for the 2020, 2016, and 2015 AP-S/URSI International Symposia. He serves as the Chair for the IEEE Northern Canada Section's Award-Winning Joint Chapter of the AP-S and MTT-S. From 2012 to 2018, he was an Associate Editor of IEEE TRANSACTIONS ON ANTENNAS AND PROPAGATION, for which he currently serves as a Track Editor. He was a Guest Editor of the Special Issue on Recent Advances in Metamaterials and Metasurfaces for IEEE TRANSACTIONS ON ANTENNAS AND PROPAGATION. He is a Registered Member of the Association of Professional Engineers and Geoscientists of Alberta.